Electronic supplementary information

Highly active ultra-fine Pd NPs confined in imine-linked COFs for nitrobenzene hydrogenation

Chunzhi Li [a,b], Xiaomin Ren [a,b], Miao Guo [a], Weijian Li [a,b], He Li [a,*], Qihua Yang [a,*]

[a] State Key Laboratory of Catalysis, Dalian Institute of Chemical Physics, Chinese Academy of Sciences, 457 Zhongshan Road, Dalian 116023, China.
[b] University of Chinese Academy of Sciences, Yuquan Road 19A, Beijing 100049, China.

Email addresses: lihe@dicp.ac.cn, yangqh@dicp.ac.cn.

Chemicals and Reagents.

All the chemicals used in this study were of analytical grade and used as received unless otherwise specified. 1,3,5-tris(p-formylphenyl)benzene (TFPB) was purchased from Jilin Chinese Academy of Sciences- Yanshen Technology Co., Ltd.

Characterizations.

The Fourier-transform infrared spectroscopy (FT-IR) spectra were recorded from 400-4000 cm^{-1} on a Nicolet Nexus 470 IR spectrometer by using KBr pellets. Solid-state ^{13}C CP-MAS NMR spectra were performed on a Bruker 500 MHz spectrometer. Liquid ^{1}H and ^{13}C NMR spectra were recorded on a Bruker Avance 400 MHz spectrometer. UV/Vis absorption spectra were recorded on SHIMADZU UV-Vis 2550 spectrophotometer. Pd content of the samples was measured by PLASAM-SPEC-II inductively coupled plasma atomic emission spectrometry (ICP-AES). X-ray powder diffraction (XRD) patterns were recorded on a Rigaku RINT D/Max-2500 powder diffraction system, equipped with Cu Kα radiation (λ = 1.54 Å). The crystalline structure of COF was resolved using powder X-ray diffraction (PXRD) combined with the computational structural simulations and Pawley refinement as conducted by Materials Studios version 8.0. Eclipsed AA stacking and staggered (AB) stacking models were built. Transmission electron microscope (TEM) characterization was undertaken using a HITACHI HT7700 microscope at an acceleration voltage of 100 kV. Before measurement, the samples were fully dispersed in ethanol and then deposited on a holey carbon film on a Cu grid. Scanning

electron microscopy (SEM) was undertaken by using a FEI Quanta 200F scanning electron microscope operating at an acceleration voltage of 20 kV. Nitrogen sorption characterization was performed on an automatic volumetric adsorption analyzer (Micromeritics ASAP2020). Before analysis, all the samples were carefully degassed at 120 $^{\circ}$C for 6 hours under the vacuum of 10 mmHg. The BET surface area was calculated from the adsorption data in a relative partial pressure (P/P_0) range of 0.04 to 0.20. The total pore volume was calculated at P/P_0 of 0.99 using a single-point adsorption value. The pore diameter was determined from the adsorption branch by using the Non Localized Density Functional Theory (NLDFT) method. X-ray photoelectron spectroscopy (XPS) was recorded on a Thermofisher ESCALAB 250Xi apparatus by using AlKα (h$_\lambda$ = 1486.6 eV) as the excitation light source. High-angle annular dark-field scanning transmission electron microscopy (HAADF-STEM) image was undertaken by using a HITACHI S5500 apparatus. CO stripping voltammetry was performed on a CH Instruments Model 760E electrochemical work station (CHI760E). The sample was dispersed in a mixture of ethanol and Nafion (5 wt% in ethanol) by sonication and then casted onto the pre-treated glassy carbon electrode (GCE) surface. The COF/GCE was served as the working electrode. A saturated calomel electrode (SCE) and a platinum wire were used as the reference and counter electrodes, respectively. For CO stripping, pure CO gas was purged through the catalyst surface, then transferring the electrodes to another cell filled with a fresh H_2SO_4 electrolyte (without CO) and purging the solution with N_2 for 15 min, after that the CO stripping was performed.

Synthesis of model compound.
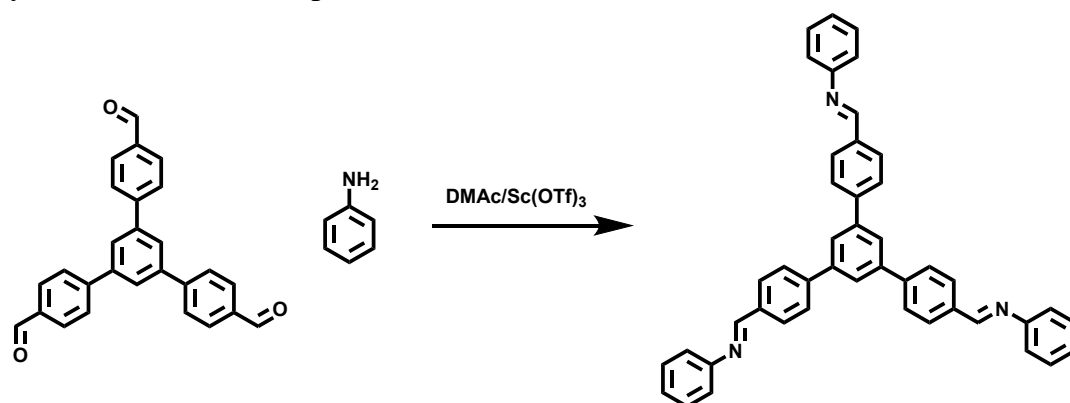
A 100 mL round bottom flask was charged with 1,3,5-tris(p-formylphenyl)benzene (0.39 g, 1 mmol), aniline (0.56 g, 6 mmol), scandium trifluoromethanesulfonate (0.03 g, 60 μmol), and dimethylacetamide (20 mL). The reaction mixture was stirred at room temperature for 12 h before being added 100 mL saturated potassium chloride solution, extracted with dichloromethane (3 x 50 mL) and washed with water (3 x 30 mL). The organic phase was then separated, dried with anhydrous sodium sulfate. The solvent was removed via rotary evaporation, and the resulting solid recrystallized in ethanol to afford product as a pale yellow solid (200 mg, 32.5%). ^{1}H-NMR (400 MHz, CDCl$_3$): δ 8.53 (s, 3H), 8.02 (d, 6H), 7.89 (s, H), 7.84 (d, 6H), 7.41 (m, 6H), 7.27 (m, 9H). ^{13}C-NMR (100 MHz, CDCl$_3$): δ 159.76, 151.97, 143.55, 141.77, 135.63, 129.42, 129.19, 127.68, 126.08, 125.65, 120.93. NMR spectra see Fig. S11 and S12.
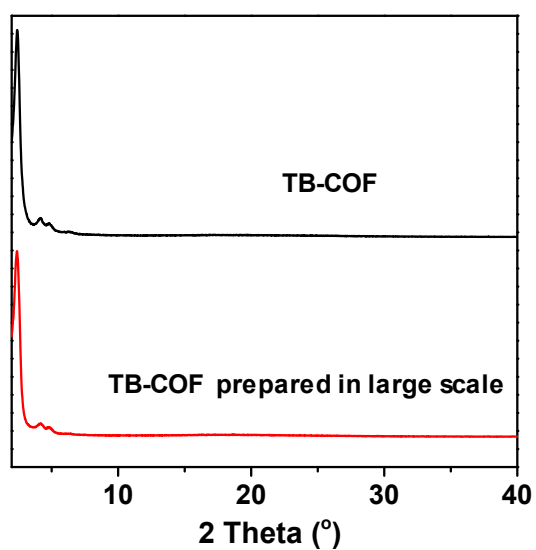
Fig. S1 PXRD patterns of TB-COF (50 mg scale) and TB-COF synthesized in large scale (500 mg).
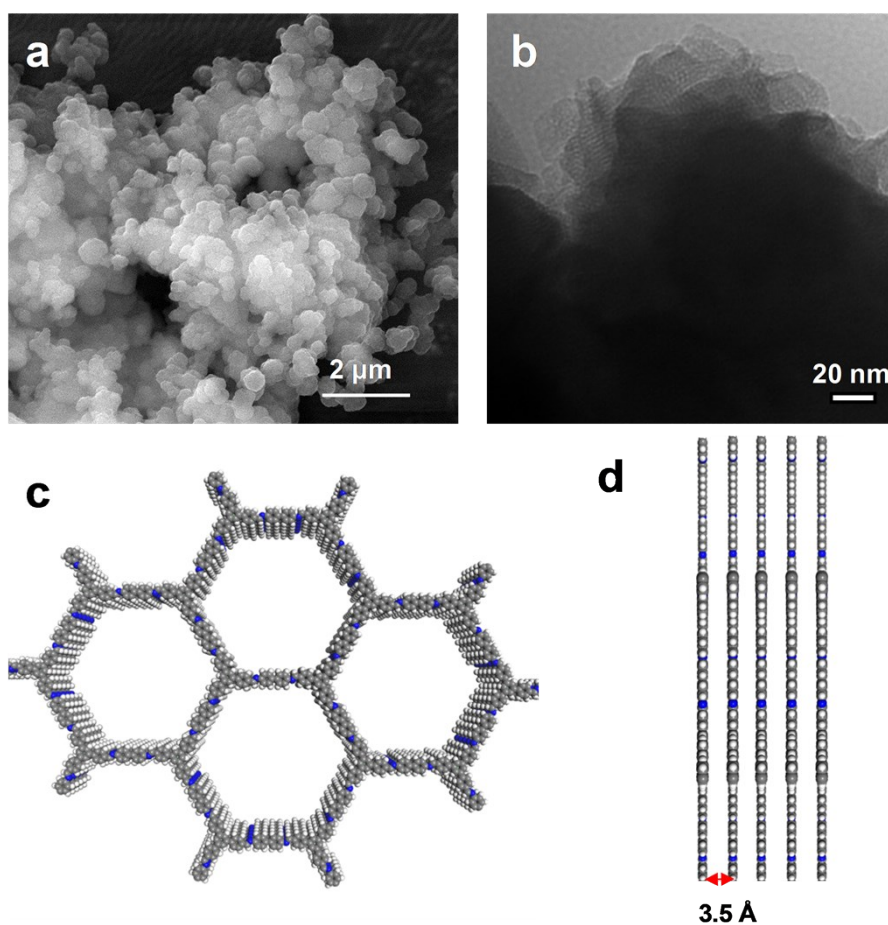

Fig. S2 (a) SEM and (b) TEM images of TB-COF, (c) top and (d) side views of the optimized structure of TB-COF.
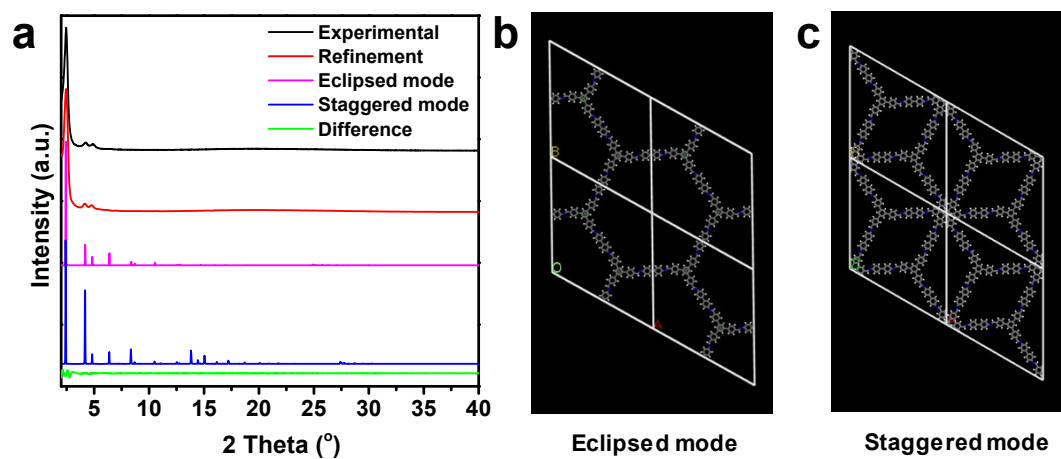
Fig. S3 (a) PXRD pattern of TB-COF: comparison between the experimental, Pawley refined and their difference, the simulated PXRD patterns using eclipsed (AA) and staggered (AB) stacking modes. (b) Eclipsed mode of TB-COF. (c) Staggered mode of TB-COF.

Table S1 Fractional atomic coordinated for unit cell of TB-COF calculated using the Materials Studio modeling program after performing the Pawley refinement.

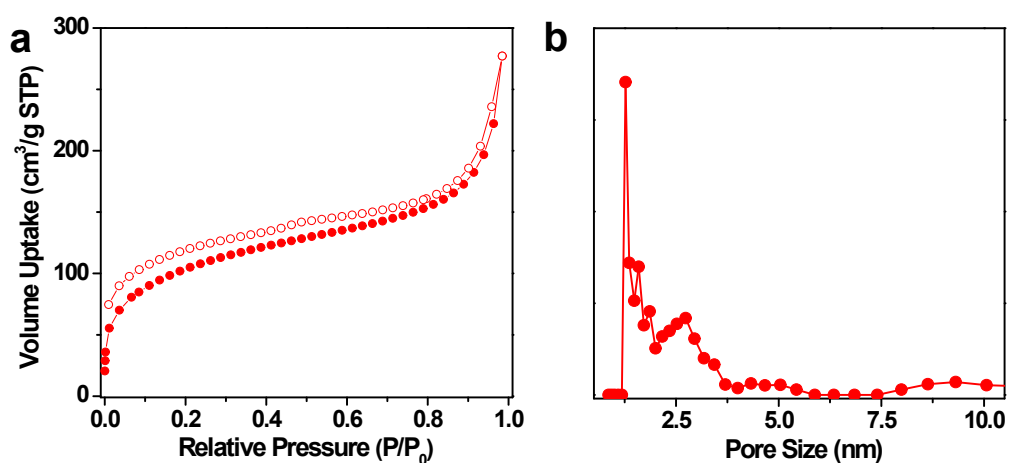| Space group		P6/M	
Calculated cell parameters		a = b = 44.473 Å, c = 3.546 Å, $\alpha = \beta = 90^\circ$, $\gamma = 120^\circ$, R_{wp} = 5.83%, R_p = 4.28%.	
atoms	x	y	z
C1	1.31992	0.6883	-0.5
C2	1.29723	0.65285	-0.5
C3	1.3794	0.7413	-0.5
C4	1.41536	0.75608	-0.5
C5	1.43704	0.79134	-0.5
C6	1.4239	0.81336	-0.5
C7	1.38861	0.79955	-0.5
C8	1.36676	0.76431	-0.5
C9	1.44733	0.85053	-0.5
N10	1.43561	0.87148	-0.5
C11	1.45303	0.54498	-0.5
C12	1.43588	0.50928	-0.5
C13	1.45406	0.49186	-0.5
C14	1.49012	0.50944	-0.5
C15	1.50682	0.54547	-0.5
C16	1.48847	0.5627	-0.5
H17	1.30971	0.70478	-0.5
H18	1.42793	0.74135	-0.5
H19	1.4643	0.80147	-0.5
H20	1.37789	0.81617	-0.5
H21	1.34012	0.75625	-0.5
H22	1.47433	0.85963	-0.5
H23	1.40849	0.49441	-0.5
H24	1.43901	0.46456	-0.5
H25	1.53406	0.5612	-0.5
H26	1.50192	0.59023	-0.5

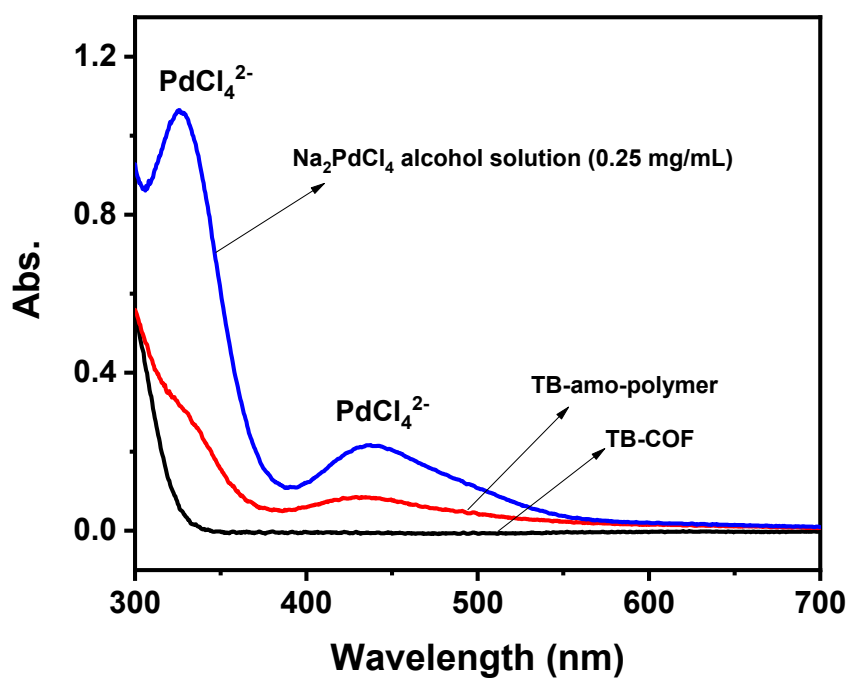**Fig. S4** (a) N_2 sorption isotherms and (b) pore size distribution of AmTB.

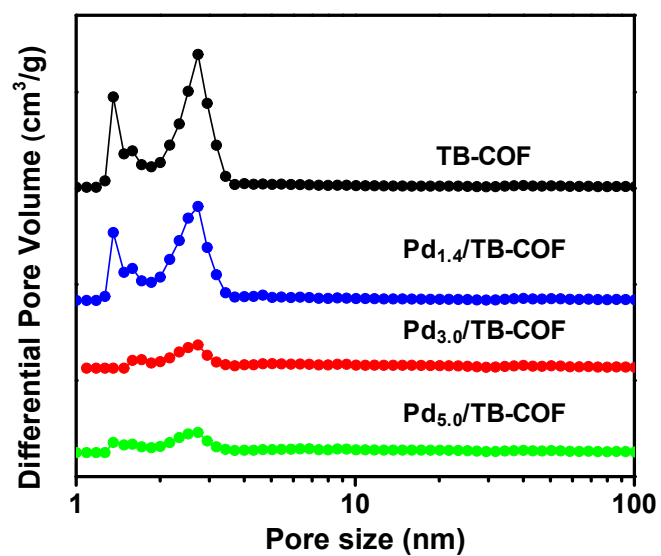**Fig. S5** The UV-vis absorption spectra of $PdCl_4^{2-}$ solution and the filtrate of TB-COF and AmTB after immersion of $PdCl_4^{2-}$ for 6 h.

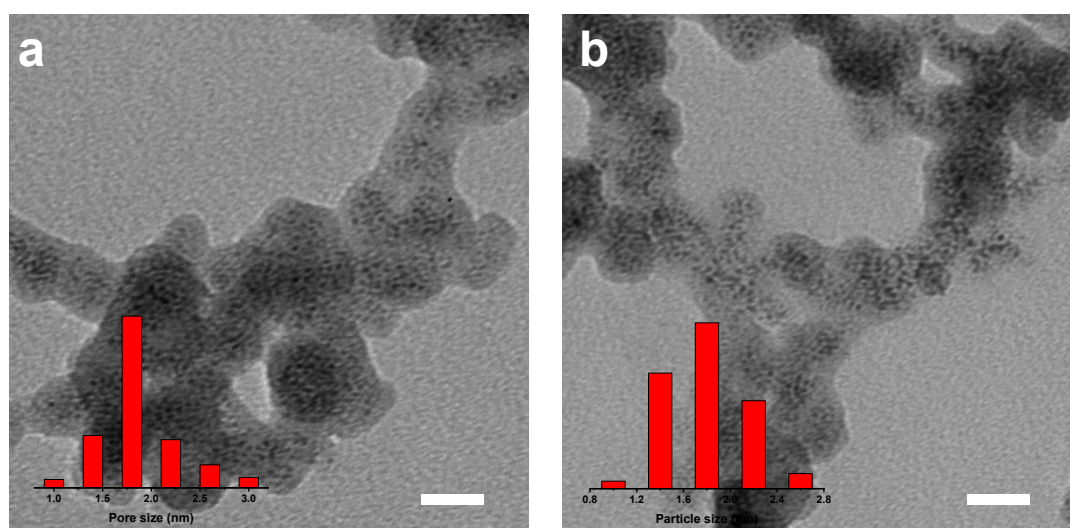**Fig. S6** Pore size distribution curves of TB-COF and Pd$_x$/TB-COF.

Fig. S7 TEM images of (a) Rh$_{5.0}$/TB-COF and (b) Pt$_{5.0}$/TB-COF (scale bar: 20 nm).
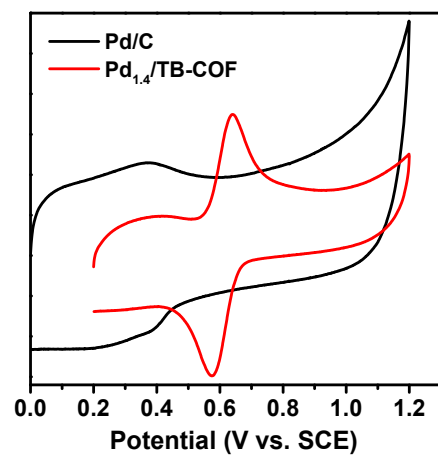
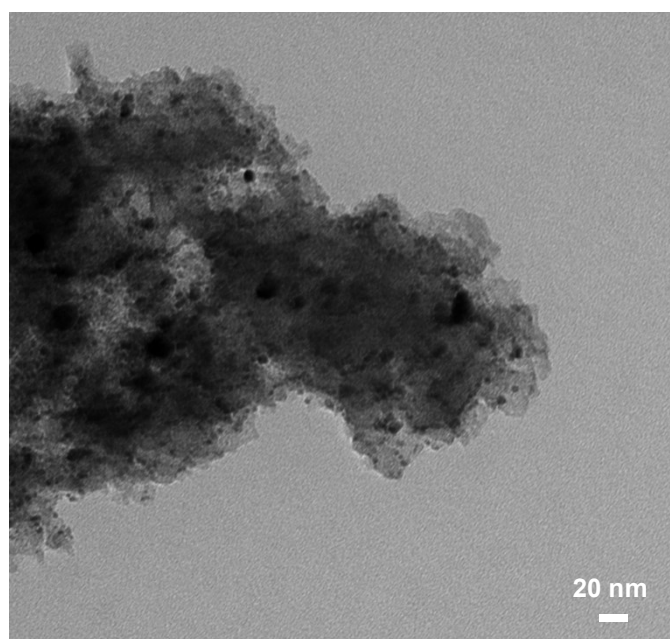**Fig. S8** CO stripping voltammetry of $Pd_{1.4}/TB\text{-}COF$ and Pd/C.

Fig. S9 TEM image of Pd/C.

Table S2. Comparison of the activity of $Pd_{1.4}$/TB-COF in nitrobenzene hydrogenation reaction with the reported polymer/MOFs based catalysts.

Catalyst	S/C	T (°C)	P (MPa)	Time (min)	Conv. (%)	Sel. (%)	TOF (h^{-1})	Ref.
$Pd_{1.4}$/TB-COF	500	RT	0.1	50	99	99	906	This work
Pd NPs incorporated in a microporous polymer with Co/C support	500	RT	0.1	120	100	100	250	1
Pd@CPP-1	200	RT	0.1	45	100	100	288	2
Pd@CPP-F1	100	40	0.15	60	100	97	114	3
Pd-H-MOF-5	100	60	0.1	90	100	100	104	4
PdNPs-PAAS	100	RT	0.1	180	100	>99	27	5
Pd-PVA	500	45	2	180	100	100	250	6
Pd@NH$_2$-HMON$_S$	50	RT	0.1	60	100	100	106	7

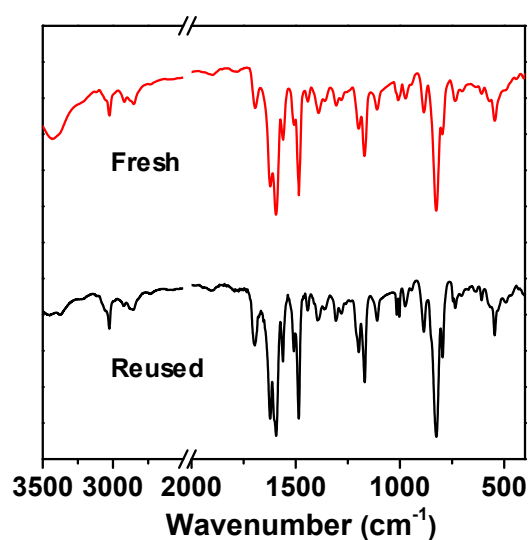**Fig. S10** FT-IR spectra of the fresh and reused $Pd_{1.4}$/TB-COF.
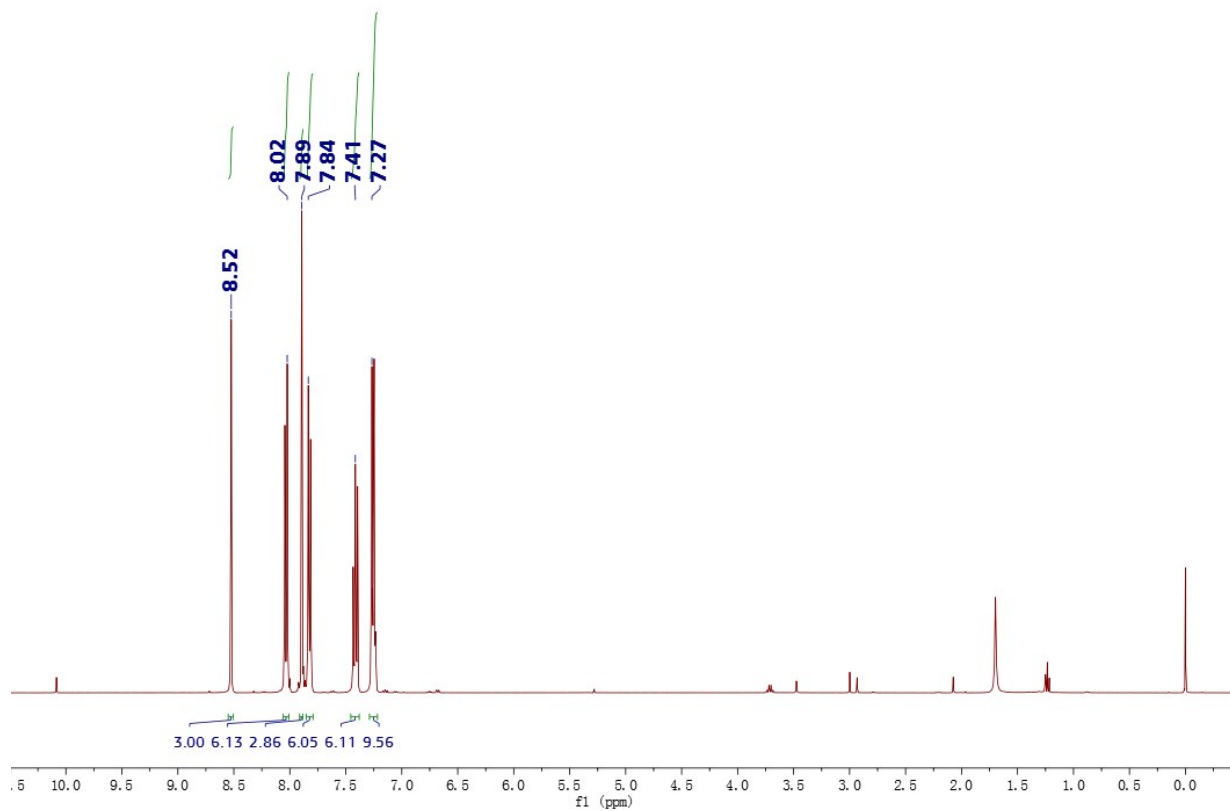
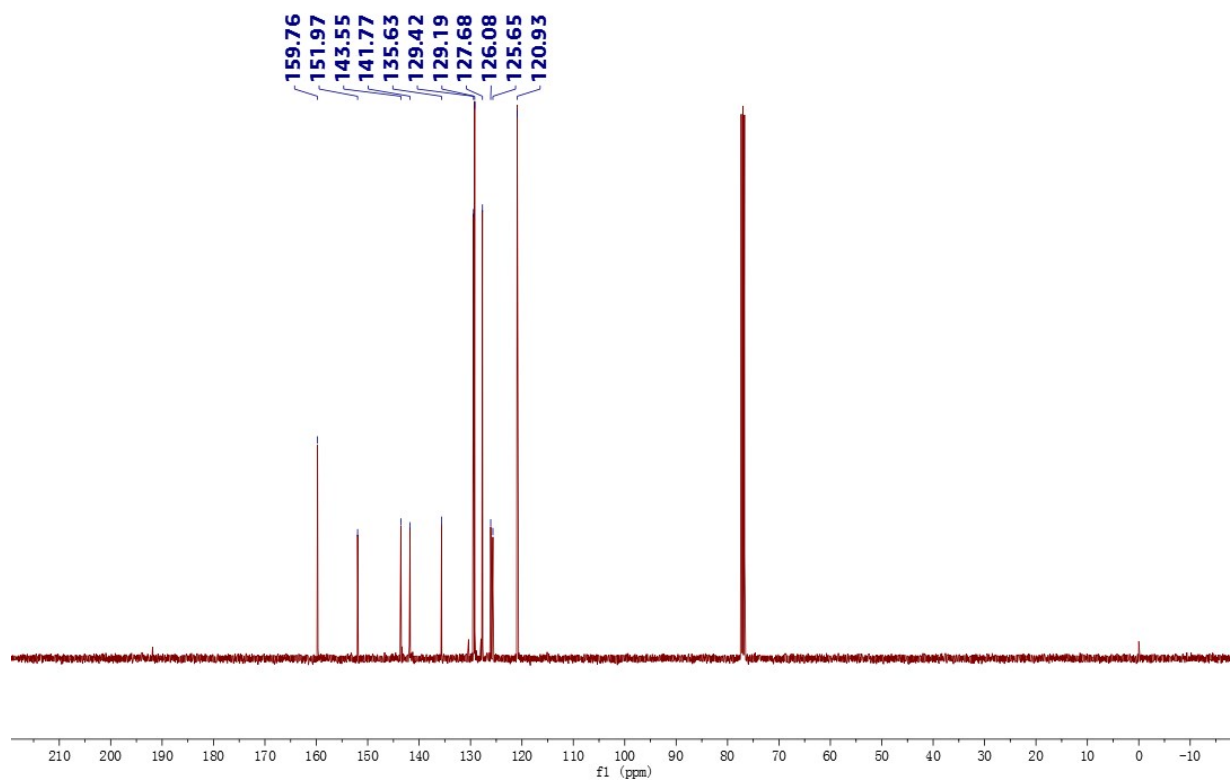**Fig. S11** ^{1}H NMR spectrum of model compound for TB-COF.

Fig. S12 ^{13}C NMR spectrum of model compound for TB-COF.

References for Supporting Information.

[1] L. Stadler, M. Homafar, A. Hartl, S. Najafishirtari, M. Colombo, R. Zboril, P. Martin, M. B. Gawande, J. Zhi and O. Reiser, *ACS Sustainable Chem. Eng.*, 2019, **7**, 2388.

[2] L. Li, H. Zhao, J. Wang and R. Wang, *ACS Nano*, 2014, **8**, 5352.

[3] L. Li, C. Zhou, H. Zhao and R. Wang, *Nano Res.*, 2015, **8**, 709.

[4] S. He, Y. Chen, Z. Zhang, B. Ni, W. He and X. Wang, *Chem. Sci.*, 2016, **7**, 7101.

[5] J. Li, Y. Wang, X. Jin, Y. Wang and H. Li, *Appl. Organometal. Chem.*, 2019, **33**, e4717.

[6] X. Wang, C. Huang, X. Li, C. Xie and S. Yu, *Chem. Asian J.*, 2019, **14**, 2266.

[7] Z. He, T. Wang, Y. Xu, M. Zhou, W. Yu, B. Shi, K. Huang, *J. Polym. Sci., Part A: Polym. Chem.*, 2018, **56**, 2045.